HHS Public Access

Author manuscript

Cell Rep. Author manuscript; available in PMC 2017 March 02.

Published in final edited form as:

Cell Rep. 2016 June 28; 16(1): 247–262. doi:10.1016/j.celrep.2016.05.053.

The Insect Prothoracic Gland as a Model for Steroid Hormone Biosynthesis and Regulation

Qiuxiang Ou[1], **Jie Zeng**[1], **Naoki Yamanaka**[2], **Christina Brakken-Thal**[3], **Michael B. O'Connor**[3], and **Kirst King-Jones**[1,*]

[1]Department of Biological Sciences, University of Alberta, G-504 Biological Sciences Building, Edmonton, AB T6G 2E9, Canada

[2]Institute for Integrative Genome Biology, Center for Disease Vector Research, and Department of Entomology, University of California, Riverside, Riverside, CA 92521, USA

[3]Department of Genetics, Cell Biology, and Development, University of Minnesota, Minneapolis, MN 55455, USA

SUMMARY

Steroid hormones are ancient signaling molecules found in vertebrates and insects alike. Both taxa show intriguing parallels with respect to how steroids function and how their synthesis is regulated. As such, insects are excellent models for studying universal aspects of steroid physiology. Here, we present a comprehensive genomic and genetic analysis of the principal steroid hormone-producing organs in two popular insect models, *Drosophila* and *Bombyx*. We identified 173 genes with previously unknown specific expression in steroid-producing cells, 15 of which had critical roles in development. The insect neuropeptide PTTH and its vertebrate counterpart ACTH both regulate steroid production, but molecular targets of these pathways remain poorly characterized. Identification of PTTH-dependent gene sets identified the nuclear receptor HR4 as a highly conserved target in both *Drosophila* and *Bombyx*. We consider this study to be a critical step toward understanding how steroid hormone production and release are regulated in all animal models.

Graphical abstract

*Correspondence: kirst.king-jones@ualberta.ca.

ACCESSION NUMBERS

The accession number for all microarray and RNA-seq data reported in this paper is Gene Expression Omnibus GEO: GSE80485.

SUPPLEMENTAL INFORMATION

Supplemental Information includes Supplemental Experimental Procedures, two figures, and eleven tables and can be found with this article online at http://dx.doi.org/10.1016/j.celrep.2016.05.053.

AUTHOR CONTRIBUTIONS

Q.O. conducted the microarray experiments, parts of the RNAi screen, and the microfluidic qPCR runs. J.Z. carried out parts of the RNAi screen and the HR4/cu experiments. N.Y. processed PG samples for RNA-seq and both N.Y. and C.B.-T. analyzed the RNA-seq data. M.B.O'C. supervised and designed the *Bombyx* experiments. K.K.-J. supervised and designed the *Drosophila* experiments, analyzed the microarray data, and wrote the manuscript.

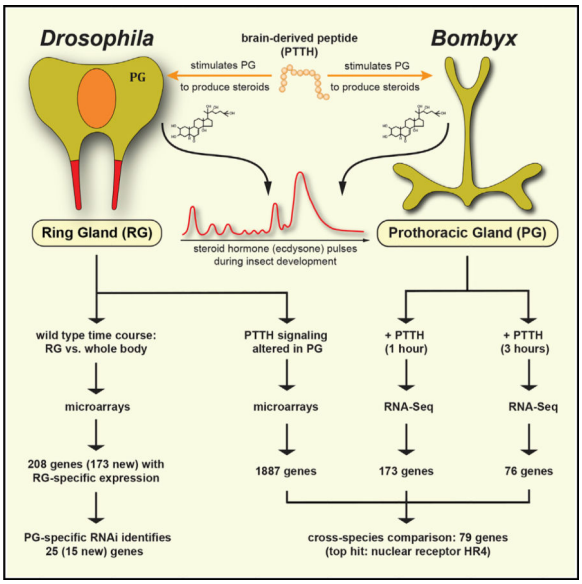

INTRODUCTION

The *Drosophila* ring gland is an emerging model for studying how endocrine glands regulate the production and release of hormones in response to developmental and environmental inputs (Yamanaka et al., 2013). In higher Diptera (*Cyclorrapha*), the ring gland (RG) is a complex endocrine structure where three endocrine glands, the corpus cardiacum (CC), corpus allatum (CA), and the prothoracic gland (PG), are fused together (Figure 1A). In other insects, including *Bombyx*, these glands form separate structures. The PG produces the molting hormones (ecdysteroids aka “ecdysone”), while the CA and CC produce the juvenile hormones and adipokinetic hormone (AKH), respectively. During *Drosophila* development, pulses of ecdysone are released from the PG (Figure 1A). The molecular actions of ecdysone through its cognate receptor, a dimer of the nuclear receptors EcR and Usp, have been studied in great detail (Koelle et al., 1991; Yao et al., 1992). However, comparatively few studies have examined the signaling pathways by which the onset, duration, and amplitude of a steroid hormone pulse are regulated.

The mechanisms by which vertebrate and insect steroidogenic cells regulate steroid hormone synthesis show intriguing parallels and homologies. In both cases, stimulation of steroid hormone production is under the control of peptide hormones released from neurons or other brain-associated cells: Ecdysone synthesis is controlled by the neuropeptide PTTH and adrenal glucocorticoids are regulated by ACTH. Human ACTH titers and transcript levels of *Drosophila* PTTH both exhibit ultradian rhythmicity, suggesting that pacemaker neurons exert temporal control over the production of these peptides in both taxa (Lightman and Conway-Campbell, 2010; McBrayer et al., 2007). Furthermore, some enzymes with key roles in the synthesis of steroid hormones are conserved between flies and mammals, such as diazepam-inhibiting protein (DIB), STARD3, and adreno-doxin reductase (AR), indicating that the synthesis of steroid hormones is an ancient invention (Freeman et al., 1999; Kolmer et al., 1994; Roth et al., 2004). Finally, vertebrate steroidogenic factor 1 (SF-1), a nuclear

receptor, transcriptionally regulates at least eight steroidogenic enzymes and appears to be required for all adrenal steroids (He et al., 2010; Sugawara et al., 1997). The *Drosophila* SF-1 ortholog, FTZ-F1, regulates at least two steroidogenic genes in the PG (Parvy et al., 2005). Taken together, key aspects of steroid hormone biosynthesis and regulation are not only conceptually similar, but also fundamentally conserved between *Drosophila* and vertebrates.

The ecdysone biosynthetic (Halloween) genes encode enzymes that convert dietary sterols to ecdysteroids such as α-ecdysone, 20-deoxymakisterone A, and 24,28-dehydromaki-sterone A (Lavrynenko et al., 2015). The best-studied biologically active ecdysteroid is 20-hydroxyecdysone (20E). In the first step of the ecdysone synthesis, pathway cholesterol is converted to 7-dehydrocholesterol (7DC) by the Neverland (Nvd) enzyme. The Halloween genes *phantom* (*phm*), *disembodied* (*dib*), *shadow* (*sad*), and *shade* (*shd*), encode cytochrome P450 hydroxylases (hereafter: P450) that carry out the last four steps toward 20E (Chávez et al., 2000; Niwa et al., 2005; Petryk et al., 2003; Warren et al., 2002, 2004). The intermediate steps that convert 7DC to 5β-ketodiol are not fully understood, however, some enzymes involved in this conversion are known and include Shroud (Sro) (Kavanagh et al., 2008; Niwa et al., 2010), Spookier (Spok) (Ono et al., 2006), and Cyp6t3 (Ou et al., 2011).

PTTH acts through the RTK Torso. Upon PTTH binding, Torso activates a small GTPase, Ras, which in turn triggers Raf/MAPK phosphorylation. This stimulates ecdysone production by upregulating specific Halloween genes, such as *dib* and *phm* (Rewitz et al., 2009). However, other components of this signaling pathway remain poorly characterized. One known target is the nuclear receptor HR4, which is negatively regulated by PTTH signaling. HR4 appears to block ecdysone biosynthesis by transcriptionally downregulating *Cyp6t3*, a PG-specific P450 enzyme(Ou et al., 2011).

In this study, we used tissue-specific microarrays to establish transcriptome profiles of the *Drosophila* RG during the last larval stage. Subsequent genetic loss-of-function studies identified genes that have never been linked to steroid hormone production. To identify genes acting downstream of the PTTH pathway, we manipulated *Drosophila* PTTH signaling via PG-specific *torso*-RNAi and expressing a constitutively active form of Ras (Ras^{V12}), followed by microarray analysis of RG samples. For *Bombyx*, we treated isolated PGs with recombinant PTTH and conducted RNA-sequencing (RNA-seq). Our results lay the foundation for interrogating conserved functions of hitherto unidentified steroidogenic players in a wide range of animal species, including humans.

RESULTS

Discovery of Genes with Specific Expression in the *Drosophila* RG

Genome-wide transcriptional profiling is routinely used for identifying tissue-specific transcripts, where the expression of an individual gene in a given tissue is compared to its average expression in the whole organism. To generate gene expression profiles from larval RGs, we analyzed four time points from third instar (L3) larvae, which represents the last larval stage before puparium formation (BPF). We chose the last larval stage for the

following reasons: (1) the RG is much bigger compared to first (L1) and second instars (L2), making dissection possible, (2) the L3 stage has three minor ecdysone pulses, while no such pulses have been reported for the first two larval stages, allowing us to correlate gene expression profiles to these pulses, (3) L3 larvae can be easily synchronized at the L2/L3 molt, since they are morphologically distinct. The four time points chosen for this analysis were 4, 8, 24, and 36 hr after the L2/L3 molt, respectively (Figure 1A). The 4 and 8 hr time points represent a time window shortly before (4 hr) or during (8 hr) the first minor ecdysone pulse when the larva determines whether it has stored sufficient nutrients to survive metamorphosis, referred to as the critical weight checkpoint (Mirth et al., 2005). We chose the 24 hr time point because it represents a feeding stage shortly after the second minor pulse, while the 36 hr time point marks the onset of wandering behavior that is likely triggered by the third minor pulse of ecdysone.

To determine whether a gene was specifically expressed in the RG, we determined the signal ratio between RG and whole body transcripts for each time point. We define here “specific expression” operationally as genes with >10-fold transcript enrichment in the RG. This is not to be confused with “exclusive” expression, rather, we expect that most genes identified by this strategy are also expressed in some other tissues. When we filtered for a >10-fold enrichment occurring at least at one of the four time points ($p < 0.01$), we identified 233 transcripts representing 208 genes (Figures 1B and 1C), of which 173 are identified here as in the RG: 22 out of 208 genes were reported in a range of publications to have specific expression in the larval RG (Figure 1B, red type), and an additional 13 genes were detected by in situ hybridization in the RG of the developing embryo by the Berkeley *Drosophila* Genome Project (BDGP, underlined in Figures 1B and 1C) (Tomancak et al., 2007). The presence of 35 previously known genes in our data demonstrated that our experimental approach was successful. For instance, we identified all known steroidogenic P450 genes with PG-specific expression, with only *Cyp6t3* missing the cutoff narrowly (9.8-fold, see Table S1).

To test the 233 RG-enriched transcripts for statistically over-represented gene ontology (GO) terms, we used the program GOSTAT (Beissbarth and Speed, 2004). The terms “oxidoreductases”, “hormone biosynthetic process”, and “sterol metabolic process” were statistically overrepresented, consistent with the fact that the RG is the principal source for steroid hormones (Table 1). The GO terms “receptor activity” and “signal transduction” were also overrepresented, indicating that a high proportion of regulatory components are devoted to coordinating the biosynthesis of endocrine signals in the RG. In addition, the GO term “tube morphogenesis” showed moderate enrichment, suggesting that gene networks controlling tube formation (as seen in trachea, salivary glands, and the heart) are similar to those utilized in the RG. This is consistent with the recent finding that tracheal and RG tissues originate from homologous precursor cells during development (Sánchez-Higueras et al., 2014). Finally, the GO terms “heat response” and “G protein-coupled receptor (GPCR) signaling pathways” were enriched due to a high proportion of genes from the HSP70 and GPCRs families, respectively (Figure 1B).

We also categorized the RG-specific transcripts according to protein function. In the “regulatory” category, which we here define to encompass transcription factors, hormones/

growth factors, kinases, receptors, and other cell signaling components, comprises nearly one third (76 in total) of the 233 transcripts with >10-fold enrichment in the RG (Figure 1B). This is consistent with the GOSTAT findings and suggests that our data can be mined to identify signaling pathways that coordinate steroidogenic and other endocrine processes in the fly. The regulatory group comprises a total of 13 DNA-binding proteins. Of these, *molting defective* (*mld*), *vvl, ouija board* (*ouib*, aka *CG11762*), *snail*, and *timeless* (*tim*) were already known to have specific expression in the RG (Cheng et al., 2014; Danielsen et al., 2014; Komura-Kawa et al., 2015; Morioka et al., 2012; Neubueser et al., 2005;Sánchez-Higueras et al., 2014), while *tinman* has been linked to the embryonic development of the CC, but no expression in the RG has been demonstrated (Park et al., 2011). Among the identified transcription factors are Escargot, which is related to Snail, and Hand, which ranks among the 50 most highly enriched mRNAs in the RG (Table S2), as well as *pdm3*, which encodes—like *vvl*—a POU-domain transcription factor.

In the "hormones and growth factor" category, we identified nine genes, of which only Akh, a glucagon-like peptide, is known to be RG-specific. Curiously, one of the peptide hormones, Ryamide (RYa), appears to act in an autocrine or paracrine manner, since its receptor RYa-R is one of the 11 GPCRs specific to the RG. We also identified spatzle5 (spz5), which acts as a neurotrophin that binds to Toll-6 and Toll-7 (McIlroy et al., 2013), but it is unclear whether these receptors function in the RG. Interestingly, two of the nine known *Drosophila* Toll-like receptor genes are expressed with high specificity in the RG, *Toll-4* and *MstProx* (Figure 1B), raising the possibility that *Drosophila* neurotrophin signaling pathways are involved in regulating hormone production.

Among the 17 transcripts that we classified as oxidoreductases, six encode known ecdysteroidogenic enzymes (Dib, Nvd, Phm, Sad, Sro, and Spok). A seventh gene, *Cyp6g2*, is specifically expressed in the CA, but not in the PG (Chung et al., 2009). Our approach identified three additional P450 genes with high RG-specific expression: *Cyp28c1, Cyp303a1*, and *Cyp6a13*, and another seven P450 genes with moderate (>2.5-fold) specificity (Table S1). We also identified Ferredoxin 2 (Fdx2), which is required for steroid synthesis, just like the vertebrate ortholog frataxin/adrenodoxin (Palandri et al., 2015).

Genes with Temporally Dynamic Expression Profiles

We next asked which genes are temporally regulated in the RG, since the L3 stage ends with a dramatic increase in steroid production to trigger the onset of metamorphosis. We limited our analysis to the 233 transcripts that are highly enriched in the RG and filtered for significant 3-fold changes in expression between any of the early (4 and 8 hr) and late (24 and 36 hr) time points. Using this strategy, we identified 21 transcripts that are downregulated, and 37 upregulated during the first 36 hr of the L3 stage. In the downregulated set are four transcription factors (CG33557, SCNF, Snail, and Tim) (Figures 2A and 2B) and a fifth gene, *escargot*, was ~2-fold reduced in expression (data not shown). None of the remaining eight RG-specific transcription factors showed temporal regulation (data not shown).

We also noted that five out of eight genes comprising the hormones and growth factor category display temporal regulation. In particular, anachronism (*ana*), a TGFβ pathway

component, is strongly downregulated as larvae progress through the L3 (Figure 2B), while *spz5, Gbp5, Pvf2*, and *RYa* are strongly upregulated during this developmental stage (Figures 2C and 2D). These data suggest that the RG produces a range of peptide hormones that show marked correlation with the onset of the metamorphosis-triggering ecdysone pulse, raising the question as to whether these signaling molecules contribute to the biosynthesis or the downstream effects of ecdysone.

We next filtered for gene expression changes during the first minor ecdysone pulse, which corresponds to the critical weight checkpoint (4 and 8 hr time points) (Figure 1A). Since the two time points are very close together, we decided to conduct two strategies. Our first approach compared two independent microarrays, one from this study and one previously published by us (Ou et al., 2011), in order to obtain a fairly stringent list (Table S3). In the second approach, we compared changes between the 4 and 8 hr time points in the RG and the whole body, but limited the analysis to microarrays from this study. This strategy allowed us to identify genes that dynamically change their expression in the RG, but not in the whole body and vice versa (Table S4). The first approach identified 42 transcripts, of which 11 were up- and 31 downregulated (Table S3). Interestingly, this set is enriched for signaling peptides, namely spatzle, spz5, SIFa, and ana, raising the possibility that these genes play a role in the critical weight checkpoint. In this light, it is noteworthy that the most strongly upregulated gene at the 8 hr time point encodes Mthl12, a GPCR for which no ligand has been described yet. The second approach also identified *mthl12* and *ana*, as they were dynamically regulated in the RG, but not in the whole body samples (Table S4).

Finally, we found that transcript levels of the ecdysteroidogenic P450 enzymes were already at very high levels in early L3 and remained at this level (Figure 2E), which seemed to contradict earlier reports showing that these genes are strongly upregulated in the late L3 (McBrayer et al., 2007; Parvy et al., 2005). We resolved this by quantitative (q)PCR, which showed that these genes are indeed upregulated (Figures 3.19 and 3.20), suggesting that the dynamic range of our microarrays was insufficient to distinguish between the very high levels in early L3 and the even further elevated levels at later time points.

Transcript Profiling over 44 hr Time Course Reveals PTTH-like Ultradian Rhythmicity

To complement our array-based gene expression profiles in the RG, we collected brain-RG complexes (BRGC) in 4 hr increments throughout the L3, resulting in 12 time points spanning nearly the entire L3 stage, representing time points from 4 hr to 48 hr after the L2/L3 molt. BRGCs can be dissected substantially easier and faster than RGs, which allowed us to increase the accuracy of the time points compared to RG samples. This detailed time course served several purposes. First, we wanted to focus on genes with established roles in ecdysone biosynthesis and build a precise transcriptional profile during the L3 stage. Second, this approach served as validation for RG-specific genes with known temporal regulation. Finally, we wanted to assess which genes are regulated with similar oscillatory patterns that were previously established for PTTH transcript levels (McBrayer et al., 2007), in an attempt to identify genes that are regulated by this pathway. In this high-throughput approach, we relied on microfluidic qPCR, and for every time point, we generated 80 data points (four biological replicates each tested in quadruplicate, all of which

were compared to five endogenous controls, 4×4×5 = 80) and plotted the median fold change in relation to the first time point (4 hr after the L2/L3 molt) as a reference.

Our strategy confirmed that PTTH transcript levels indeed oscillated (Figure 3.1), however, here we found that expression of PTTH peaked with a 12–16 hr periodicity, whereas our previous report indicated an 8 hr oscillatory pattern (McBrayer et al., 2007). In total, 15 of the interrogated 26 genes oscillated in a more or less comparable pattern to that of PTTH itself, matching at least two of the three PTTH pulses, namely at 12, 20–24, and 40–44 hr after the molt (Figures 3.1–3.16). Two genes, *tim* (Figure 3.26) and *Cyp18a1* (Figure 3.27) showed no obvious correlation to any of the three PTTH peaks, while all other genes had at least one peak that corresponded to the PTTH oscillations.

It is interesting to note that the regulation of the Halloween genes appears to fall into two different classes. Class I, composed of *nvd, spok*, and *sad*, along with the PTTH receptor gene *torso* and a key transcription factor required for ecdysone biosynthesis encoded by *E75* (Bialecki et al., 2002; Cáceres et al., 2011), is defined by remarkably similar expression profiles: Class I genes display three distinct expression peaks that correlate nicely with the three PTTH peaks (the third peak being delayed). All genes are only moderately (2- to 8-fold) induced toward the end of the L3, with little or no regression at late L3 stages (Figures 3.10–3.14). In contrast, genes of class II, which comprised *dib, phm*, and *sro*, lacked the distinct first two peaks found in class I and only correlated with the major PTTH peak at 40–44 hr. All were dramatically upregulated relative to the 4 hr time point (40- to 180 -fold), however, this was followed by a decrease in expression at late L3 stages (Figures 3.19–3.21). These data suggest that each of two Halloween gene classes are coordinately regulated, where class I displays tight temporal control by the PTTH pathway, while class II seems to respond with dramatic upregulation, but only during the late larval PTTH surge.

We included another 11 non-Halloween P450 genes in our analysis, because they displayed moderate to high transcript enrichment in the RG (Table S1). One exception was *Cyp4g1*, which we included because transcripts of this gene were reported to be enriched in the RG relative to the larval CNS (Niwa et al., 2011). None of these 11 P450 genes exhibited any similarity to the expression profiles of class I and II Halloween genes. For four of these uncharacterized P450 genes, we conducted in situ hybridization, which confirmed their specific expression in the RG (Figure 4B). Further, it appears that *Cyp317a1, Cyp6a13*, and *Cyp12e1* formed a distinct set (Figures 3.2–3.4) that displayed minor, but significant, expression changes that closely resembled the PTTH profile. *Cyp303a1* and *Cyp6g2* lacked a pronounced response to the third PTTH peak (Figures 3.5 and 3.7), while *Cyp6t3, Cyp6v1*, and *Cyp4g1* (Figures 3.8, 3.17, and 3.23) were first downregulated before being moderately induced toward the late L3 stage. Finally, *Cyp28c1, Cyp6a14*, and *Cyp18a1* (Figures 3.18, 3.24, and 3.27) were strongly downregulated in late L3, but their overall patterns were distinct enough to make coordinate regulation of this set unlikely. Taken together, while additional non-Halloween P450 genes were expressed in the RG, they were distinct from the classic Halloween genes, which, as we show here, fall into two separate classes.

Tissue-Specific and Whole Body RNAi Screen

We next tested whether the RG-specific transcripts are functionally important. For this, we screened the top 102 genes—defined by transcript enrichment in the RG—via RNAi (Table S5), which included genes that have already confirmed functions in the PG. We used three RG Gal4 drivers, thus interfering with gene function in either the PG (*phm22-Gal4*), the CA (*Aug21-Gal4*), or the CC (*Akh-Gal4*). We also carried out a control cross with a strong ubiquitous driver, *actin-Gal4*, which we reasoned would reveal whether the RNAi line was functional through developmental phenotypes or increased lethality (Tables S6 and S7).

Nearly all (25 out 26) genes were identified by PG-specific RNAi. We found only one hit for the CA, caused by a knock down of *Oatp74D*, which encodes an organic anion transporter (Table 2). We identified no hits for the CC, consistent with the finding that ablation of this gland did not cause lethality (Kim and Rulifson, 2004; Lee and Park, 2004). In Figure 4A, we show examples of the major phenotypic classes caused by RNAi in the PG: The most common developmental defect was a large body phenotype, which we observed for 21 out of 25 genes. One line exhibited embryonic lethality (Ugt37c1), four lines died as large first instar (L1) larvae (Npc1a, sro, vvl, and phm), and three lines arrested development as large L2 larvae (Hsp70Ba, Rgk1, and CG11762/ouib) (Table 2). Overall, only two lines displayed a normal body size (*MstProx* and *Mes2*) and one, *curled* (*cu*), resulted in a smaller body size (Figure 4C). The large body phenotype is typically caused by prolonged feeding times when the molt to a larva or pupa is delayed or blocked, a commonly observed phenotype in larvae with defects in ecdysone production and/or release (Colombani et al., 2005; Mirth et al., 2005; Rewitz et al., 2009; Yamanaka et al., 2013, 2015). On the other hand, a smaller body size may indicate a premature attempt to pupariate, thus reducing feeding times (King-Jones et al., 2005; Ou et al., 2011).

The main function of the PG is to produce ecdysteroids during the larval stages. We therefore asked whether supplementing media with 20E would rescue at least some of the RNAi phenotypes. In case of *phm>Ugt37c1*-RNAi, which was embryonic lethal, we soaked embryos in a buffer containing 20E, while all other RNAi lines received 20E through feeding. Of all 25 *phm*>RNAi lines tested, we observed partial rescue in 14 lines, which we defined as either reaching the next developmental stage and/or restoring a normal body size due to a rescue of developmental timing (Table 2). We observed a complete rescue (where most animals reach the adult stage) in seven of the lines (*CG30471, dib, phm, sad, sro, spok*, and *spz5*) and no rescue for four of the genes (*cu, Mes2, MstProx*, and *Ugt37c1*).

We were curious about the unusual phenotype seen in the *phm>cu*-RNAi larvae, since it was very similar to what we reported for loss-of-*HR4* function (King-Jones et al., 2005; Ou et al., 2011). Given that HR4 represents a known transcription factor target of the PTTH pathway, we wondered whether *cu* and *HR4* are functionally linked.

Loss-of-*cu* Function Accelerates Development

Since this study found that nuclear receptor HR4 is a highly conserved target of PTTH signaling (see last section), we were curious as to whether the smaller body size observed in *phm>cu*-RNAi animals (Figure 4C) was caused by developmental acceleration, a phenotype

we observed in *Drosophila HR4* mutants and *HR4*-RNAi animals (King-Jones et al., 2005; Ou et al., 2011). This was indeed the case. Disrupting *cu* or *HR4* function via RNAi in the RG or the PG reduced the duration of larval development in both genotypes by 10 (Figure 4D) or 7 hr (data not shown), respectively. *Drosophila* CU is orthologous to vertebrate Nocturnin (NOC), a circadian rhythm effector protein (Grönke et al., 2009). Interestingly, NOC interacts with the nuclear receptor PPARγ to facilitate its translocation to the nucleus, raising the possibility that a similar interaction may occur between CU and HR4. Consistent with this, PPARγ and HR4 are the only known nuclear receptors where a MAP kinase regulates their access to the nucleus (Burgermeister et al., 2007;Kawai et al., 2010). To explore a possible interaction between *cu* and *HR4*, we expressed an HR4 cDNA in the RG, which causes L3 arrest due to its ability to block ecdysone synthesis upon entry into the nucleus (Ou et al., 2011). If CU facilitated nuclear entry of HR4, then HR4-mediated lethality should be reduced in a CU-depleted background. Indeed, when we expressed *HR4* in a *cu* null mutant (cu^3), animals were substantially healthier and now developed to the pupal stage (Figure 4E). We also carried out the reverse test. This was possible because expression of a *cu* cDNA resulted in L2 arrest, which we reasoned was caused by facilitating nuclear access of HR4 and thus causing a reduction in ecdysone synthesis. Consistent with the above result, overexpression of *cu* in a *phm>HR4*-RNAi background rescued ~20% of the larval population to the L3 stage of which another 1% reached the pupal stage (Figure 4F). This genetic interaction, in combination with the phenotypic similarity, supports the idea that *Drosophila* CU is a component of the HR4 signaling mechanism. Finally, we tested whether *Cyp6t3*, which is repressed when HR4 is nuclear, would be de-repressed in a CU-depleted background (= decreased nuclear access of HR4). Indeed, we saw moderate, but significant, upregulation of *Cyp6t3* in early L3 *phm>cu*-RNAi larvae (Figure 4G). Taken together, these data suggested that our screen identified *cu* as a component of the PTTH-HR4 axis, but future studies are needed to establish this at the molecular level.

Genes Functioning Downstream of PTTH in *Drosophila*

Based on our time course analysis of key components of the ecdysone biosynthetic pathway, we concluded that the PTTH signaling pathway governs the expression of many genes in the PG (Figure 3). To examine this observation in a more direct manner, we manipulated the PTTH/Torso/Ras signaling pathway by genetic means and examined the genome-wide responses by carrying out RG-specific microarrays. In particular, we chose to ectopically express a constitutively active form of Ras, Ras^{V12}, in the PG. In a separate experiment, we targeted Torso function via RNAi in the PG. We then examined these lines, including controls, at two developmental stages during the L3, namely at the beginning and the middle of the wandering stage when PTTH transcripts levels are low and high, respectively, corresponding to −18 and −8 hr BPF in controls (Figure 1A). The staging of the larval populations was based on the blue gut method (Andres and Thummel, 1994), which allowed us to compensate for differences in developmental timing incurred by the various genetic backgrounds used in this approach.

We mined the data by several means. First, we asked which genes are up- or downregulated between the early (−18 hr BPF) and the late wandering stage (−8 hr BPF). We reasoned that this represented low and high endogenous PTTH levels respectively (in controls), and we

thus searched for genes that failed to be up- or downregulated in *phm>torso*-RNAi larvae. This strategy yielded 42 transcripts that were up- and 45 transcripts that were downregulated in a *torso*-dependent manner (Tables S8A and S8B). The overall trend was that genes upregulated in controls were more dramatically upregulated in Ras^{V12} animals (37 out of 42 transcripts) and showed reduced expression in *phm>torso*-RNAi larvae (Figures 5A–5D), consistent with the idea that upregulation of these genes occurred in response to PTTH. Notably, upregulation of *HR4* was completely abolished in *phm>torso*-RNAi larvae, suggesting that PTTH also exerts transcriptional control over *HR4* (Figures 5B and S2B; Table S10). In total, 98 out the 233 RG-specific transcripts (42%) were affected by either RAS^{V12} or *torso*-RNAi (Figure 5I). This included *CG9541, CG30438*, and *Traf4*, which all exhibited strong dependency on Torso or Ras (Figures 5A, 5C, and S2B). Genes that were downregulated in controls showed the inverse trend (38 out of 45 transcripts), namely lower expression in response to RAS^{V12} and higher expression in *phm>torso*-RNAi animals (Figures 5E–5H). Indeed, one would expect that genes upregulated by PTTH activity would follow this exact trend by showing elevated expression when Ras is constitutively active and reduced transcript levels when the Torso function is disrupted; and one would expect the inverse trend for downregulated genes.

A significant set of 62 transcripts was upregulated by Ras^{V12}, but downregulated in *torso*-RNAi. The reverse comparison yielded only 29 genes, which was not significant (Figure 5J). This suggests that the PTTH/Torso/Ras pathway acts largely by upregulating target gene expression, rather than exerting negative control.

RNA-Seq of PTTH-Treated *Bombyx* PGs

Lastly, we aimed to complement our genome-wide analysis of PTTH signaling by conducting RNA-seq of PTTH-treated PGs of the silkworm *Bombyx mori*. In particular, we dissected *Bombyx* PGs from day 4 fifth (last) instar larvae and treated them with or without recombinant PTTH for either 1 or 3 hr, after which the glands were collected to prepare total RNA for RNA-seq. The disadvantage of manipulating the PTTH/Torso/Ras signaling cassette by genetic means (in *Drosophila*) is that it perturbs the pathway throughout development, which inevitably causes secondary effects. In contrast, in vitro stimulation of the PGs with recombinant PTTH holds the advantage of identifying genes that display rapid changes in expression levels within the first few hours after PTTH treatment. For this approach, we used *Bombyx* larvae, since it is currently the only insect species where both the whole genome sequence and recombinant PTTH are available, making it feasible to conduct RNA-seq of isolated PGs treated with PTTH in vitro. The absence of recombinant PTTH and the technical unfeasibility of dissecting PGs from *Drosophila* make it currently impossible to conduct the same experiment in this species.

We identified 173 and 76 genes that were either up- or down-regulated after 1 or 3 hr of treatment with PTTH, respectively (Table S9). The list of upregulated genes contains all the P450 genes that were previously shown to be transcriptionally responsive to PTTH, namely *dib, phm, spook*, and *Cyp4g25* (Niwa et al., 2005, 2011; Yamanaka et al., 2007), thus validating our approach. Moreover, most of the identified genes have predicted fly orthologs (Table S9), allowing us to compare these PTTH-responsive genes to fly genes we

identified by genetic manipulation of the PTTH signaling pathway (Tables S8A, S8B, and S10). We used two approaches to compare the *Bombyx* and *Drosophila* data sets. First, we compared all *Drosophila* genes that were significantly up- or downregulated in a *torso*-dependent manner (Tables S8A and S8B) to the *Bombyx* results. Using this highly selective strategy, only a single gene, *Hr4*, was common to both sets. In both cases, *HR4* was upregulated in a PTTH/Torso-dependent manner (Tables S8A and S9A), indicating that HR4 is transcriptionally induced by PTTH during the last larval stage prior to the onset of metamorphosis, consistent with the strong increase of HR4 transcripts we observed in the L3 time course analysis (Figure 3.22).

Our second strategy identified *Drosophila* genes that were affected by altering PTTH signaling based on whether they showed significant changes in their profiles at either of the two time points between controls and the Ras^{V12} or *torso*-RNAi data sets (2-fold change + ANOVA, $p < 0.05$) to the *Bombyx* PTTH data. This approach identified 79 *Drosophila* genes that, like their *Bombyx* counterparts, responded to changes in PTTH signaling (Table S10). This list includes the nuclear receptors HR4 and Eip75B, the P450 genes *Cyp4g15, dib*, and *Cyp18a1*, and nutritional regulators including cabut and InR (insulin receptor). This suggested that while the genes acting downstream of PTTH in *Bombyx* and *Drosophila* have diverged substantially, there is a core set of genes, such as HR4, E75, and ecdysteroidogenic enzymes that are common targets of this pathway and likely conserved in most insect species.

DISCUSSION

In this study, we aimed at the following objectives: (1) identification of genes with specific expression in the *Drosophila* RG; (2) finding genes with likely roles in steroid hormone synthesis; (3) discovering signaling pathways and transcriptional regulators that control steroid production; (4) examining the molecular responses to PTTH signaling, a key regulator of insect steroid production; and (5) identifying conserved genes that act downstream of PTTH signaling in two model insect species.

We identified 208 genes (233 transcripts) with specific expression in the RG. Our decision to consider a >10-fold transcript enrichment compared to the whole body sample was arbitrary, but resulted in a sensible gene set that reflected biological relevance (233 transcripts). For instance, a 5-fold cutoff would have resulted in 745 transcripts, while a 20-fold threshold would have shortened the list to 109. Well-characterized genes with known expression in the RG, such as *torso, cu, NPC1a, Cyp6g2*, and *Akh* all displayed >10-fold transcript enrichment. However, a few genes with known RG-specific expression missed the cutoff. This included *Cyp6t3* (FC 9.8) and *start1* (FC 9.0), which encode a putative intracellular sterol transporter (Roth et al., 2004). No other P450 gene (other than *Cyp6t3*) was found in the 5- to 10-fold cohort, suggesting that a >10-fold cutoff was reasonable.

Identification of P450 Genes Required for Ecdysone Synthesis

Our array and in situ data identified several P450 genes with hitherto unknown roles in the *Drosophila* RG, while our approach in *Bombyx* only identified P450 enzymes with known roles in insect steroidogenesis. Of the three P450 genes uncovered specifically by this study

with high RG specificity (*Cyp6a13, Cyp303a1*, and *Cyp28c1*) only one—*Cyp28c1*—resulted in a discernible RNAi phenotype with *phm22-Gal4*. A previous study reported no expression of *Cyp28c1* in the RG, (Chung et al., 2009), however, this is easily reconciled because *Cyp28c1* transcript levels are low only in the second half of the L3 (Figures 2B and 3.18), corresponding to the time point used in the study. *Cyp28c1* is a predicted target of the Snail (Halfon et al., 2008; The modENCODE Consortium et al., 2010), consistent with the finding that both have similar profiles (Figure 2B). Two other P450 genes with known roles in ecdysone are also predicted targets of Snail, *sad*, and *Cyp18a1*, suggesting that this transcription factor has a yet to be elucidated role in the regulation of insect steroidogenesis. *Cyp18a1* is, just like *Cyp28c1*, downregulated during the course of the L3 stage (Figure 3.27), supporting the idea that both are regulated by Snail. A significant set of non-enriched P450 transcripts have similar profiles to that of *Cyp28c1* and *Cyp18a1* (Figure S1B), raising the possibility that some of these genes are coordinately regulated.

Strong transcript enrichment in the RG is not necessarily a required feature for a P450 gene's participation in ecdysone production: We identified a series of moderately expressed P450 genes (Table S1), some of which we validated via in situ hybridization to confirm their expression in the RG (Figure 4B). To identify other potentially relevant P450 genes, we compared P450 profiles in a developmental time course and compared their profiles to that of PTTH (Figure 3). While this approach is limited due to the fact that we used BRGCs rather than isolated RGs as sample material, it did allow us to query multiple, tightly controlled time points and should be adequate to test whether genes correlate with the PTTH profile. Using this strategy, we identified eight P450 genes (*dib, spok, sad, phm, sro, Cyp6t3, Cyp6v1*, and *Cyp4g1*) that displayed moderate to strong upregulation in late L3 stages, consistent with the idea that this is mediated by PTTH (Figure 3).

Finally, one important finding of this study was that the classic Halloween genes displayed extremely high transcript abundance throughout the L3 stage, in fact, so high that the microarray signal was saturated, giving the false impression of a "flat" profile for the duration of the L3 (Figure 2E). Previous studies examining Halloween gene expression during larval development showed strong upregulation toward later L3 stages (Anderson et al., 1996; McBrayer et al., 2007; Parvy et al., 2005), which we confirmed here for *dib, phm*, and *sro*, while *nvd, spok*, and *sad* show only moderate increases in transcript levels. However, strong upregulation does not equal low absolute levels prior to induction, rather, our array data demonstrated that Halloween transcripts are highly abundant in early L3, long before transcript levels rise. Thus, qPCR data can be misleading, given that genes like *phm* are nearly 200-fold induced during the L3, despite the fact that *phm* levels are already high at the 4 hr time point (compare Figures 3.20 to 2E). Similarly, antibody stains and in situ hybridizations can be equally misleading, because these reactions can be stopped at any time. We conclude that while transcriptional upregulation is an important factor in the regulation of steroidogenic genes, other signaling mechanisms are likely in place that contribute to the formation of a steroid pulse, such as the regulation of ecdysone secretion from the PG (Yamanaka et al., 2015).

Transcription Factors Regulating Steroid Production

Our array data identified eight transcription factors with previously unknown roles in the RG (Figure 1B). Interestingly, both Hand and Tinman have been linked to heart development in the fly, while Snail and Escargot have redundant functions in the wing disc, are co-expressed in embryonic and wing disc tissue, and have been shown to genetically interact, raising the possibility that Escargot and Snail act in concert in the RG (Ashraf et al., 1999; Cai et al., 2001). Snail binds to several nuclear receptor genes, including *HR4* (Figure S2), *FTZ-F1, Eip75B*, and *HR3*, all of which have been shown to have roles in the regulation of ecdysone production. Interestingly, chromatin immunoprecipitation (ChIP)-seq data showed that Tinman binds to *snail, Hand*, and *Traf4* (Halfon et al., 2008; The modENCODE Consortium et al., 2010), all of which have specific expression in the RG (Figure S2).

HR4 is a prime example for a transcription factor that shows no transcript enrichment in the RG, but appears to be a key regulator of PTTH signaling in both *Bombyx* and *Drosophila*. Our study found that *Bombyx* HR4 was highly inducible by recombinant PTTH, consistent with its strong upregulation during the last larval stage in *Drosophila* (Figure 3.22), which was dependent on Torso function (Figures 5B and S2). This suggests a model where PTTH/Torso controls *HR4* transcriptionally, as shown by this study, as well as at the protein level, shown by our earlier work (Ou et al., 2011). In this study, we identified a potential partner for HR4, the CU protein (aka Curled aka NOC), because RNAi against either *cu* or *HR4* caused developmental acceleration. The two genes interacted in various genetic combinations, and the validity of the RNAi lines was confirmed via ubiquitous expression of the *cu*-RNAi via *actin-Gal4*, which resulted in a phenocopy of the null mutation: curled wings (Table S6). In addition, vertebrate NOC facilitates nuclear entry of nuclear receptor PPARγ, suggesting that this function is conserved in *Drosophila*, but acts on HR4, consistent with the fact that flies do not have an ortholog of PPARγ. CU itself appears to be controlled by PTTH/Torso (Figure 5H), suggesting that an intricate regulatory network controls the activity of HR4.

In summary, this study has unearthed a plethora of uncharacterized genes that function in the PG and act downstream of the PTTH signaling pathway. Given the intriguing parallels to vertebrate steroid physiology, our data provides a platform that allows a detailed comparison between insect and vertebrate endocrinology from a molecular and cell signaling perspective. As such, this study should pave the way for future studies that utilize the insect PG as a model for studying the biology of steroid hormones in particular and endocrine systems in general.

EXPERIMENTAL PROCEDURES

Drosophila Stocks

We obtained w^{1118} (#3605) and *Sgs3-GFP* (#5884) from the Bloomington *Drosophila* stock center. RNAi lines used in our RNAi screens were acquired from the Vienna *Drosophila* Resource Center (VDRC), and all IDs are listed in Tables 2 and S5, S6, and S7. The cu^3 allele was a kind gift from Ronald K€uhnlein. We used the following Gal4 drivers for the PG: *phm22-Gal4* (Rewitz et al., 2009); the CA: *Aug21-Gal4/CyO, act-GFP* (Siegmund and

Korge, 2001); the CC: *AKH-Gal4* (Rhea et al., 2010); the RG: *P0206-Gal4* (Zhou et al., 2004); and ubiquitous expression: *actin5C-Gal4/CyO, act-GFP* (Struhl and Basler, 1993). Flies were reared on standard agar-cornmeal medium at 25°C (with or without 0.05% bromophenol blue).

Sample Preparation and Microarrays

Flies (w^{1118}) were raised at 25°C and larvae were carefully staged at the L2/L3 molt. We collected ten RGs per sample to keep the time window for dissection below 30 min. RGs were dissected in PBS, rinsed briefly, and immediately transferred to TRIzol reagent (Invitrogen) for RNA isolation. Since *torso*-RNAi and Ras^{V12} affected developmental timing, we used relative staging by rearing larvae on standard medium supplemented with 0.05% bromophenol blue to monitor developmental stages based on gut coloring (Andres and Thummel, 1994). RGs were dissected from control ($phmw^{1118}$) larvae at 30 hr after the molt (blue gut = −18 hr BPF) and 40 hr after the molt (partial blue gut = −8 hr BPF) (Figure 1). To obtain similarly staged *torso*-RNAi and Ras^{V12} larvae, we collected larvae with comparable gut staining, thus adjusting for differences in absolute time relative to controls. RGs were transferred to TRIzol reagent for RNA extraction and sample preparation for microarray analysis was carried out as described earlier (Ou et al., 2011).

RNAi Screen

Eight *phm22-Gal4* virgin females were crossed to five or six males of a given RNAi stock. Three replicates were generated from each cross and reared at 25°C until scoring. $phm>w^{1118}$ was used as a negative control. All crosses were maintained on standard agar-cornmeal medium at 25°C.

20E Rescue Experiments

20E (Cat. No. 7980-000) was purchased from Steraloids and 10 mg/ml ethanol stock was stored at −20°C. Standard cornmeal-agar medium was supplemented with 0.33 mg/ml of the hormone or an equivalent amount of ethanol. For rescue experiments, embryos were collected in 2 hr intervals and reared on 20E-supplemented medium or control medium w/o 20E. $phm>w^{1118}$ was used as a control.

Microfluidic qPCR Analysis

Larval populations for the 4–24 hr time points were staged once at the L2/L3 molt, while we re-synchronized larvae for later time points based on visual appearance of *Sgs3-GFP* (Warren et al., 2006). Flies were entrained under a 12 hr light/dark cycle at 25°C and 70% humidity for 3 days. We dissected ten BRGCs in PBS per sample (four biological replicates for each time point), followed by RNA isolation in 100 μl TRIzol and RNeasy purification (QIAGEN). RNA concentrations were measured with a NanoDrop 1000 Spectrophotometer (Thermo Scientific), and RNA integrity was evaluated using Agilent RNA Nano Chips. cDNA synthesis was performed with the ABI High-Capacity cDNA Synthesis Kit (Cat. No. 4368814). For cDNA pre-amplification, an equivalent of 5 ng of total RNA was used to amplify each cDNA sample with the TaqMan PreAmp 2X Master Mix (Applied Biosystems, Part No. 4384266) following the manufacturer's instructions (BioMark, Fluidigm). High-

throughput qPCR (9,216 reactions per run)was performed as described earlier (Bujold et al., 2010).

In Situ RNA Hybridization

We carried out in situ hybridizations as previously described (Ou et al., 2011), and all primers used for probe generation are listed in Table S11.

Statistics and Data Mining

For the analysis of *Drosophila* Nimblegen microarrays, including ANOVA, t tests, differential expression, and generation of heatmaps, we used the RMA-based Arraystar 4.0 (DNAStar) (Irizarry et al., 2003). Filtering for p values and fold changes, as well as gene set comparisons for Venn diagrams are based on ACCESS (Microsoft). Calculation of fold changes were based on geometric means of individual samples. Chi-square tests for Venn diagrams were calculated in Excel.

Supplementary Material

Refer to Web version on PubMed Central for supplementary material.

Acknowledgments

The authors thank the Bloomington *Drosophila* Stock Center at Indiana University and the VDRC for sending fly stocks. We also thank the lab of Hiroshi Kataoka for generously providing recombinant *Bombyx* PTTH and Roland Kühnlein for sending the cu^3 stock. We extend our thanks to Adam Magico for testing the RNAi lines in the corpora cardiaca and Heather McDermid for critical comments on the manuscript. K.K.-J. is supported by the CIHR (MOP 93761) and the NSERC of Canada (RGPIN 341543). N.Y. is supported by NIH grant R00 HD073239 from the Eunice Kennedy Shriver National Institute of Child Health and Human Development (NICHD). Finally, M.B.O'C. receives funding from the National Institute of General Medical Sciences (R01 GM093301) in support of this work.

REFERENCES

Anderson MG, Certel SJ, Certel K, Lee T, Montell DJ, Johnson WA. Function of the Drosophila POU domain transcription factor drifter as an upstream regulator of breathless receptor tyrosine kinase expression in developing trachea. Development. 1996; 122:4169–4178. [PubMed: 9012536]

Andres, AJ., Thummel, CS. Methods for Quantitative Analysis of Transcription in Larvae and Prepupae. Goldstein, LSB., Fyrberg, EA., editors. New York: Academic Press; 1994. p. 565-573.

Ashraf SI, Hu X, Roote J, Ip YT. The mesoderm determinant snail collaborates with related zinc-finger proteins to control Drosophila neurogenesis. EMBO J. 1999; 18:6426–6438. [PubMed: 10562554]

Beissbarth T, Speed TP. GOstat: find statistically overrepresented Gene Ontologies within a group of genes. Bioinformatics. 2004; 20:1464–1465. [PubMed: 14962934]

Bialecki M, Shilton A, Fichtenberg C, Segraves WA, Thummel CS. Loss of the ecdysteroid-inducible E75A orphan nuclear receptor uncouples molting from metamorphosis in *Drosophila*. Dev. Cell. 2002; 3:209–220. [PubMed: 12194852]

Bujold M, Gopalakrishnan A, Nally E, King-Jones K. Nuclear receptor DHR96 acts as a sentinel for low cholesterol concentrations in Drosophila melanogaster. Mol. Cell. Biol. 2010; 30:793–805. [PubMed: 19933845]

Burgermeister E, Chuderland D, Hanoch T, Meyer M, Liscovitch M, Seger R. Interaction with MEK causes nuclear export and downregulation of peroxisome proliferator-activated receptor gamma. Mol. Cell. Biol. 2007; 27:803–817. [PubMed: 17101779]

Cáceres L, Necakov AS, Schwartz C, Kimber S, Roberts IJ, Krause HM. Nitric oxide coordinates metabolism, growth, and development via the nuclear receptor E75. Genes Dev. 2011; 25:1476–1485. [PubMed: 21715559]

Cai Y, Chia W, Yang X. A family of snail-related zinc finger proteins regulates two distinct and parallel mechanisms that mediate Drosophila neuroblast asymmetric divisions. EMBO J. 2001; 20:1704–1714. [PubMed: 11285234]

Chávez VM, Marqués G, Delbecque JP, Kobayashi K, Hollingsworth M, Burr J, Natzle JE, O'Connor MB. The Drosophila disembodied gene controls late embryonic morphogenesis and codes for a cytochrome P450 enzyme that regulates embryonic ecdysone levels. Development. 2000; 127:4115–4126. [PubMed: 10976044]

Cheng C, Ko A, Chaieb L, Koyama T, Sarwar P, Mirth CK, Smith WA, Suzuki Y. The POU factor ventral veins lacking/Drifter directs the timing of metamorphosis through ecdysteroid and juvenile hormone signaling. PLoS Genet. 2014; 10:e1004425. [PubMed: 24945490]

Chung H, Sztal T, Pasricha S, Sridhar M, Batterham P, Daborn PJ. Characterization of Drosophila melanogaster cytochrome P450 genes. Proc. Natl. Acad. Sci. USA. 2009; 106:5731–5736. [PubMed: 19289821]

Colombani J, Bianchini L, Layalle S, Pondeville E, Dauphin-Villemant C, Antoniewski C, Carré C, Noselli S, Léopold P. Antagonistic actions of ecdysone and insulins determine final size in Drosophila. Science. 2005; 310:667–670. [PubMed: 16179433]

Danielsen ET, Moeller ME, Dorry E, Komura-Kawa T, Fujimoto Y, Troelsen JT, Herder R, O'Connor MB, Niwa R, Rewitz KF. Transcriptional control of steroid biosynthesis genes in the Drosophila prothoracic gland by ventral veins lacking and knirps. PLoS Genet. 2014; 10:e1004343. [PubMed: 24945799]

Freeman MR, Dobritsa A, Gaines P, Segraves WA, Carlson JR. The *dare* gene: steroid hormone production, olfactory behavior, and neural degeneration in *Drosophila*. Development. 1999; 126:4591–4602. [PubMed: 10498693]

Grönke S, Bickmeyer I, Wunderlich R, Jäckle H, Kühnlein RP. Curled encodes the Drosophila homolog of the vertebrate circadian deadenylase Nocturnin. Genetics. 2009; 183:219–232. [PubMed: 19581445]

Halfon MS, Gallo SM, Bergman CM. REDfly 2.0: an integrated database of cis-regulatory modules and transcription factor binding sites in Drosophila. Nucleic Acids Res. 2008; 36:D594–D598. [PubMed: 18039705]

He J, Cheng Q, Xie W. Minireview: Nuclear receptor-controlled steroid hormone synthesis and metabolism. Mol. Endocrinol. 2010; 24:11–21. [PubMed: 19762543]

Irizarry RA, Hobbs B, Collin F, Beazer-Barclay YD, Antonellis KJ, Scherf U, Speed TP. Exploration, normalization, and summaries of high density oligonucleotide array probe level data. Biostatistics. 2003; 4:249–264. [PubMed: 12925520]

Kavanagh KL, Jörnvall H, Persson B, Oppermann U. Medium- and short-chain dehydrogenase/reductase gene and protein families: the SDR superfamily: functional and structural diversity within a family of metabolic and regulatory enzymes. Cell. Mol. Life Sci. 2008; 65:3895–3906. [PubMed: 19011750]

Kawai M, Green CB, Lecka-Czernik B, Douris N, Gilbert MR, Kojima S, Ackert-Bicknell C, Garg N, Horowitz MC, Adamo ML, et al. A circadian-regulated gene, Nocturnin, promotes adipogenesis by stimulating PPAR-gamma nuclear translocation. Proc. Natl. Acad. Sci. USA. 2010; 107:10508–10513. [PubMed: 20498072]

Kim SK, Rulifson EJ. Conserved mechanisms of glucose sensing and regulation by Drosophila corpora cardiaca cells. Nature. 2004; 431:316–320. [PubMed: 15372035]

King-Jones K, Charles JP, Lam G, Thummel CS. The ecdysone-induced DHR4 orphan nuclear receptor coordinates growth and maturation in Drosophila. Cell. 2005; 121:773–784. [PubMed: 15935763]

Koelle MR, Talbot WS, Segraves WA, Bender MT, Cherbas P, Hogness DS. The Drosophila EcR gene encodes an ecdysone receptor, a new member of the steroid receptor superfamily. Cell. 1991; 67:59–77. [PubMed: 1913820]

Kolmer M, Roos C, Tirronen M, Myöhänen S, Alho H. Tissue-specific expression of the diazepam-binding inhibitor in Drosophila melanogaster: cloning, structure, and localization of the gene. Mol. Cell. Biol. 1994; 14:6983–6995. [PubMed: 7935415]

Komura-Kawa T, Hirota K, Shimada-Niwa Y, Yamauchi R, Shimell M, Shinoda T, Fukamizu A, O'Connor MB, Niwa R. The Drosophila zinc finger transcription factor ouija board controls ecdysteroid biosynthesis through specific regulation of spookier. PLoS Genet. 2015; 11:e1005712. [PubMed: 26658797]

Lavrynenko O, Rodenfels J, Carvalho M, Dye NA, Lafont R, Eaton S, Shevchenko A. The ecdysteroidome of Drosophila: influence of diet and development. Development. 2015; 142:3758–3768. [PubMed: 26395481]

Lee G, Park JH. Hemolymph sugar homeostasis and starvation-induced hyperactivity affected by genetic manipulations of the adipokinetic hormone-encoding gene in Drosophila melanogaster. Genetics. 2004; 167:311–323. [PubMed: 15166157]

Lightman SL, Conway-Campbell BL. The crucial role of pulsatile activity of the HPA axis for continuous dynamic equilibration. Nat. Rev. Neurosci. 2010; 11:710–718. [PubMed: 20842176]

McBrayer Z, Ono H, Shimell M, Parvy J-P, Beckstead RB, Warren JT, Thummel CS, Dauphin-Villemant C, Gilbert LI, O'Connor MB. Prothoracicotropic hormone regulates developmental timing and body size in *Drosophila*. Dev. Cell. 2007; 13:857–871. [PubMed: 18061567]

McIlroy G, Foldi I, Aurikko J, Wentzell JS, Lim MA, Fenton JC, Gay NJ, Hidalgo A. Toll-6 and Toll-7 function as neurotrophin receptors in the Drosophila melanogaster CNS. Nat. Neurosci. 2013; 16:1248–1256. [PubMed: 23892553]

Mirth C, Truman JW, Riddiford LM. The role of the prothoracic gland in determining critical weight for metamorphosis in Drosophila melanogaster. Curr. Biol. 2005; 15:1796–1807. [PubMed: 16182527]

Morioka E, Matsumoto A, Ikeda M. Neuronal influence on peripheral circadian oscillators in pupal *Drosophila* prothoracic glands. Nat. Commun. 2012; 3:909. [PubMed: 22713751]

Neubueser D, Warren JT, Gilbert LI, Cohen SM. *molting defective* is required for ecdysone biosynthesis. Dev. Biol. 2005; 280:362–372. [PubMed: 15882578]

Niwa R, Sakudoh T, Namiki T, Saida K, Fujimoto Y, Kataoka H. The ecdysteroidogenic P450 Cyp302a1/disembodied from the silkworm, Bombyx mori, is transcriptionally regulated by prothoracicotropic hormone. Insect Mol. Biol. 2005; 14:563–571. [PubMed: 16164612]

Niwa R, Namiki T, Ito K, Shimada-Niwa Y, Kiuchi M, Kawaoka S, Kayukawa T, Banno Y, Fujimoto Y, Shigenobu S, et al. *Non-molting glossy/shroud* encodes a short-chain dehydrogenase/reductase that functions in the 'Black Box' of the ecdysteroid biosynthesis pathway. Development. 2010; 137:1991–1999. [PubMed: 20501590]

Niwa R, Sakudoh T, Matsuya T, Namiki T, Kasai S, Tomita T, Kataoka H. Expressions of the cytochrome P450 monooxygenase gene Cyp4g1 and its homolog in the prothoracic glands of the fruit fly Drosophila melanogaster (Diptera: Drosophilidae) and the silkworm Bombyx mori (Lepidoptera: Bombycidae). Appl. Entomol. Zool. (Jpn.). 2011; 46:533–543.

Ono H, Rewitz KF, Shinoda T, Itoyama K, Petryk A, Rybczynski R, Jarcho M, Warren JT, Marqués G, Shimell MJ, et al. Spook and Spookier code for stage-specific components of the ecdysone biosynthetic pathway in Diptera. Dev. Biol. 2006; 298:555–570. [PubMed: 16949568]

Ou Q, Magico A, King-Jones K. Nuclear receptor DHR4 controls the timing of steroid hormone pulses during *Drosophila* development. PLoS Biol. 2011; 9:e1001160. [PubMed: 21980261]

Palandri A, L'hôte D, Cohen-Tannoudji J, Tricoire H, Monnier V. Frataxin inactivation leads to steroid deficiency in flies and human ovarian cells. Hum. Mol. Genet. 2015; 24:2615–2626. [PubMed: 25628335]

Park S, Bustamante EL, Antonova J, McLean GW, Kim SK. Specification of *Drosophila* corpora cardiaca neuroendocrine cells from mesoderm is regulated by Notch signaling. PLoS Genet. 2011; 7:e1002241. [PubMed: 21901108]

Parvy JP, Blais C, Bernard F, Warren JT, Petryk A, Gilbert LI, O'Connor MB, Dauphin-Villemant C. A role for betaFTZ-F1 in regulating ecdysteroid titers during post-embryonic development in Drosophila melanogaster. Dev. Biol. 2005; 282:84–94. [PubMed: 15936331]

Petryk A, Warren JT, Marqués G, Jarcho MP, Gilbert LI, Kahler J, Parvy JP, Li Y, Dauphin-Villemant C, O'Connor MB. Shade is the Drosophila P450 enzyme that mediates the hydroxylation of ecdysone to the steroid insect molting hormone 20-hydroxyecdysone. Proc. Natl. Acad. Sci. USA. 2003; 100:13773–13778. [PubMed: 14610274]

Rewitz KF, Yamanaka N, Gilbert LI, O'Connor MB. The insect neuropeptide PTTH activates receptor tyrosine kinase torso to initiate metamorphosis. Science. 2009; 326:1403–1405. [PubMed: 19965758]

Rhea JM, Wegener C, Bender M. The proprotein convertase encoded by amontillado (amon) is required in Drosophila corpora cardiaca endocrine cells producing the glucose regulatory hormone AKH. PLoS Genet. 2010; 6:e1000967. [PubMed: 20523747]

Roth GE, Gierl MS, Vollborn L, Meise M, Lintermann R, Korge G. The Drosophila gene Start1: a putative cholesterol transporter and key regulator of ecdysteroid synthesis. Proc. Natl. Acad. Sci. USA. 2004; 101:1601–1606. [PubMed: 14745013]

Sánchez-Higueras C, Sotillos S, Castelli-Gair Hombría J. Common origin of insect trachea and endocrine organs from a segmentally repeated precursor. Curr. Biol. 2014; 24:76–81. [PubMed: 24332544]

Siegmund T, Korge G. Innervation of the ring gland of Drosophila melanogaster. J. Comp. Neurol. 2001; 431:481–491. [PubMed: 11223816]

Struhl G, Basler K. Organizing activity of wingless protein in Drosophila. Cell. 1993; 72:527–540. [PubMed: 8440019]

Sugawara T, Kiriakidou M, McAllister JM, Holt JA, Arakane F, Strauss JF 3rd. Regulation of expression of the steroidogenic acute regulatory protein (StAR) gene: a central role for steroidogenic factor 1. Steroids. 1997; 62:5–9. [PubMed: 9029708]

The modENCODE Consortium. et al. Identification of functional elements and regulatory circuits by Drosophila modENCODE. Science. 2010; 330:1787–1797. [PubMed: 21177974]

Tomancak P, Berman BP, Beaton A, Weiszmann R, Kwan E, Hartenstein V, Celniker SE, Rubin GM. Global analysis of patterns of gene expression during Drosophila embryogenesis. Genome Biol. 2007; 8:R145. [PubMed: 17645804]

Warren JT, Petryk A, Marques G, Jarcho M, Parvy JP, Dauphin-Villemant C, O'Connor MB, Gilbert LI. Molecular and biochemical characterization of two P450 enzymes in the ecdysteroidogenic pathway of Drosophila melanogaster. Proc. Natl. Acad. Sci. USA. 2002; 99:11043–11048. [PubMed: 12177427]

Warren JT, Petryk A, Marqués G, Parvy JP, Shinoda T, Itoyama K, Kobayashi J, Jarcho M, Li Y, O'Connor MB, et al. Phantom encodes the 25-hydroxylase of Drosophila melanogaster and Bombyx mori: a P450 enzyme critical in ecdysone biosynthesis. Insect Biochem. Mol. Biol. 2004; 34:991–1010. [PubMed: 15350618]

Warren JT, Yerushalmi Y, Shimell MJ, O'Connor MB, Restifo LL, Gilbert LI. Discrete pulses of molting hormone, 20-hydroxyecdysone, during late larval development of Drosophila melanogaster: correlations with changes in gene activity. Dev. Dyn. 2006; 235:315–326. [PubMed: 16273522]

Yamanaka N, Honda N, Osato N, Niwa R, Mizoguchi A, Kataoka H. Differential regulation of ecdysteroidogenic P450 gene expression in the silkworm, Bombyx mori. Biosci. Biotechnol. Biochem. 2007; 71:2808–2814. [PubMed: 17986773]

Yamanaka N, Rewitz KF, O'Connor MB. Ecdysone control of developmental transitions: lessons from Drosophila research. Annu. Rev. Entomol. 2013; 58:497–516. [PubMed: 23072462]

Yamanaka N, Marqués G, O'Connor MB. Vesicle-mediated steroid hormone secretion in Drosophila melanogaster. Cell. 2015; 163:907–919. [PubMed: 26544939]

Yao TP, Segraves WA, Oro AE, McKeown M, Evans RM. Drosophila ultraspiracle modulates ecdysone receptor function via heterodimer formation. Cell. 1992; 71:63–72. [PubMed: 1327536]

Zhou X, Zhou B, Truman JW, Riddiford LM. Overexpression of broad: a new insight into its role in the *Drosophila* prothoracic gland cells. J. Exp. Biol. 2004; 207:1151–1161. [PubMed: 14978057]

In Brief

Little is known about how steroidogenesis is regulated in animals. Here, Ou et al. examine the steroid hormone-producing cells from two popular insect models to identify players that act in the synthesis and regulation of steroids. The nuclear receptor HR4 is identified as a key regulator in both systems.

Highlights

- Identification of 173 genes with specific expression in steroidogenic cells
- *Drosophila* steroidogenic cells have high proportion of signaling pathway components
- In vivo RNAi screen identifies 15 genes involved in steroid production and regulation
- Candidate targets of neuropeptide PTTH in controlling steroidogenesis are described

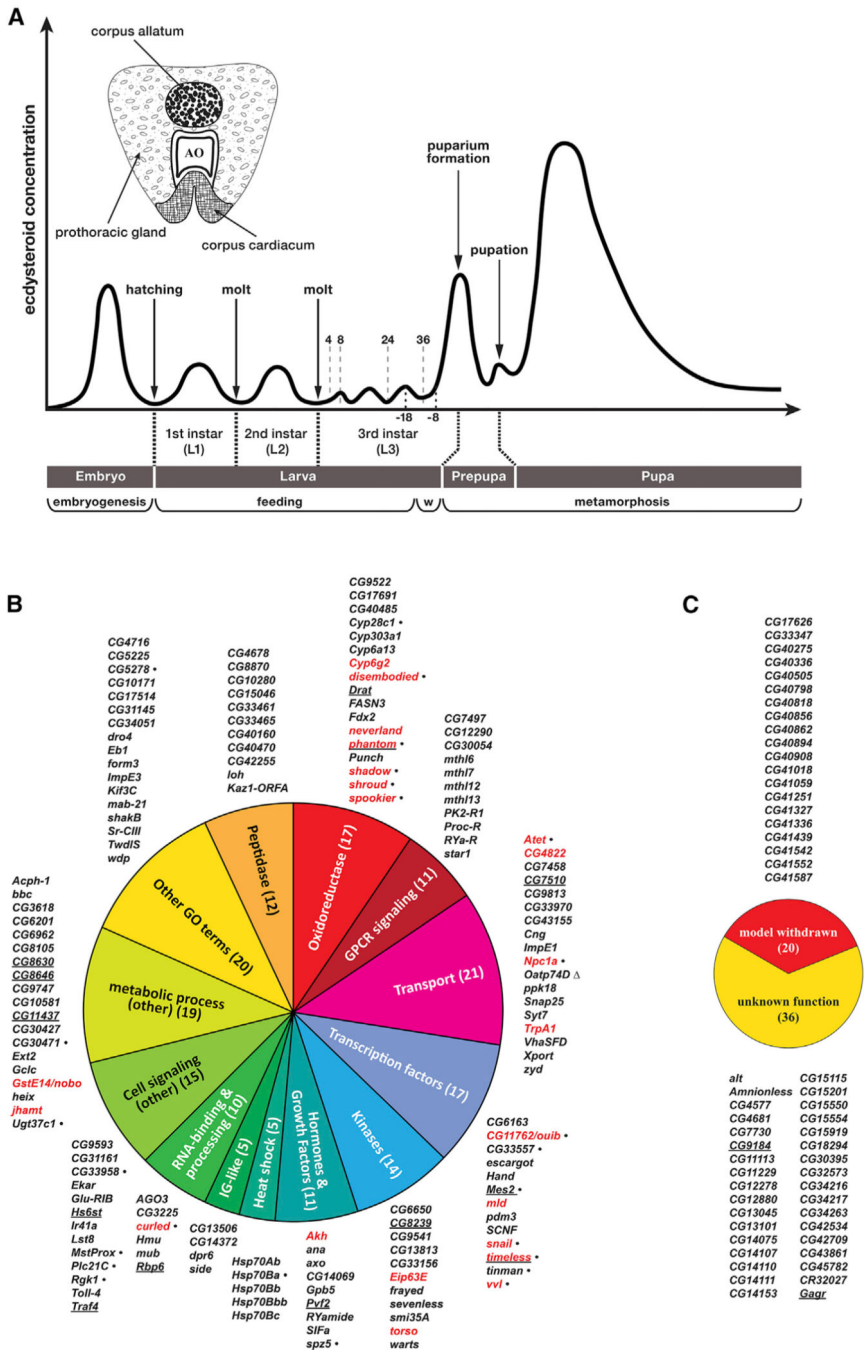

Figure 1. RG Overview and Transcript Enrichment

(A) The *Drosophila* RG surrounds the aorta (AO) and comprises three glands, the CA, the CC, and the PG, which produces ecdysone. Major pulses of ecdysone trigger all developmental transitions including hatching, the two larval molts, puparium formation, and metamorphosis. The three minor pulses during the L3 stage are linked to (1) critical weight checkpoint, (2) glue gene induction, and (3) wandering behavior (w). The 4, 8, 24, and 36 indicate hr after the L2/L3 molt at which wild-type RGs were dissected. The −18 and −8

represent hr before puparium formation (BPF), at which we collected RGs for the *RAS*^{V12}/*torso*-RNAi microarrays.

(B and C) Classification of 233 RG-specific transcripts (B and C). The numbers in brackets represent the number of transcripts. The red font represents genes where prior reports found specific expression in the larval RG. The underlined genes were found to be specifically expressed in the embryonic RG based on work from the BDGP (Tomancak et al., 2007). The dots indicate PG-specific RNAi hits found in this study, while the single triangle indicates a CA-specific hit (see Table 2).

(B) 177 of the 233 transcripts (representing 154 genes) with >10-fold enrichment in the RG were classifiable based on GO terms and/or protein domains.

(C) 56 transcripts (54 genes) have no known function or are not currently assigned to a gene model.

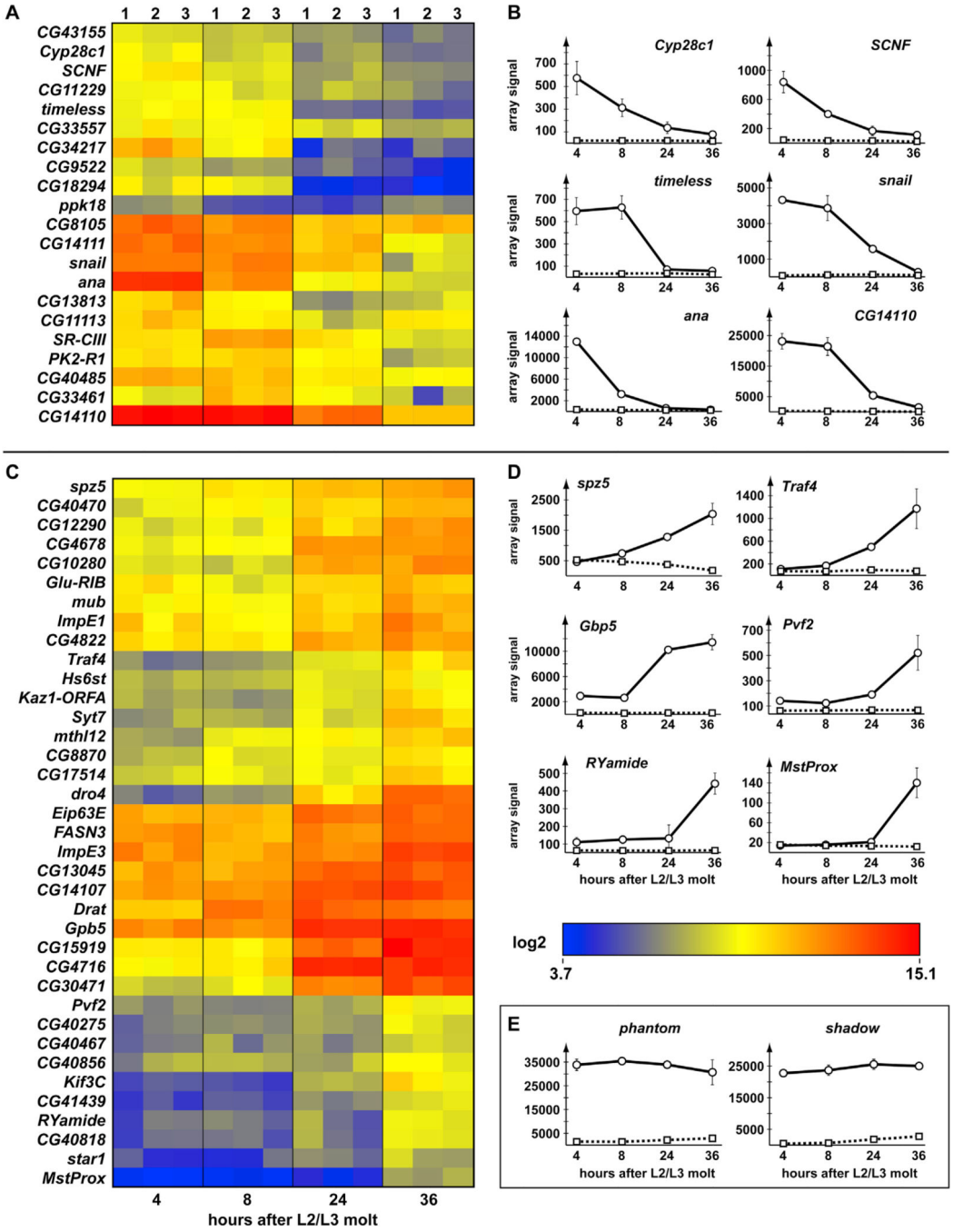

Figure 2. Transcripts with Dynamic Profiles during the L3 Stage

Among the set of 233 RG-specific transcripts, we identified 37 up- and 21 downregulated transcripts.

(A and C) Heatmaps for down- (A) and upregulated genes (C). The numbers at the top reflect biological replicates for microarrays 1–3 and the numbers at the bottom are hours since the molt to L3.

(B and D) Temporal profiles for six down- (B) and six upregulated genes (D).

(E) Shows two highly expressed steroidogenic genes *phm* and *sad*. The y axis represents average array signal (black line: RG signal and dotted line: whole body signal). The error bars represent SD.

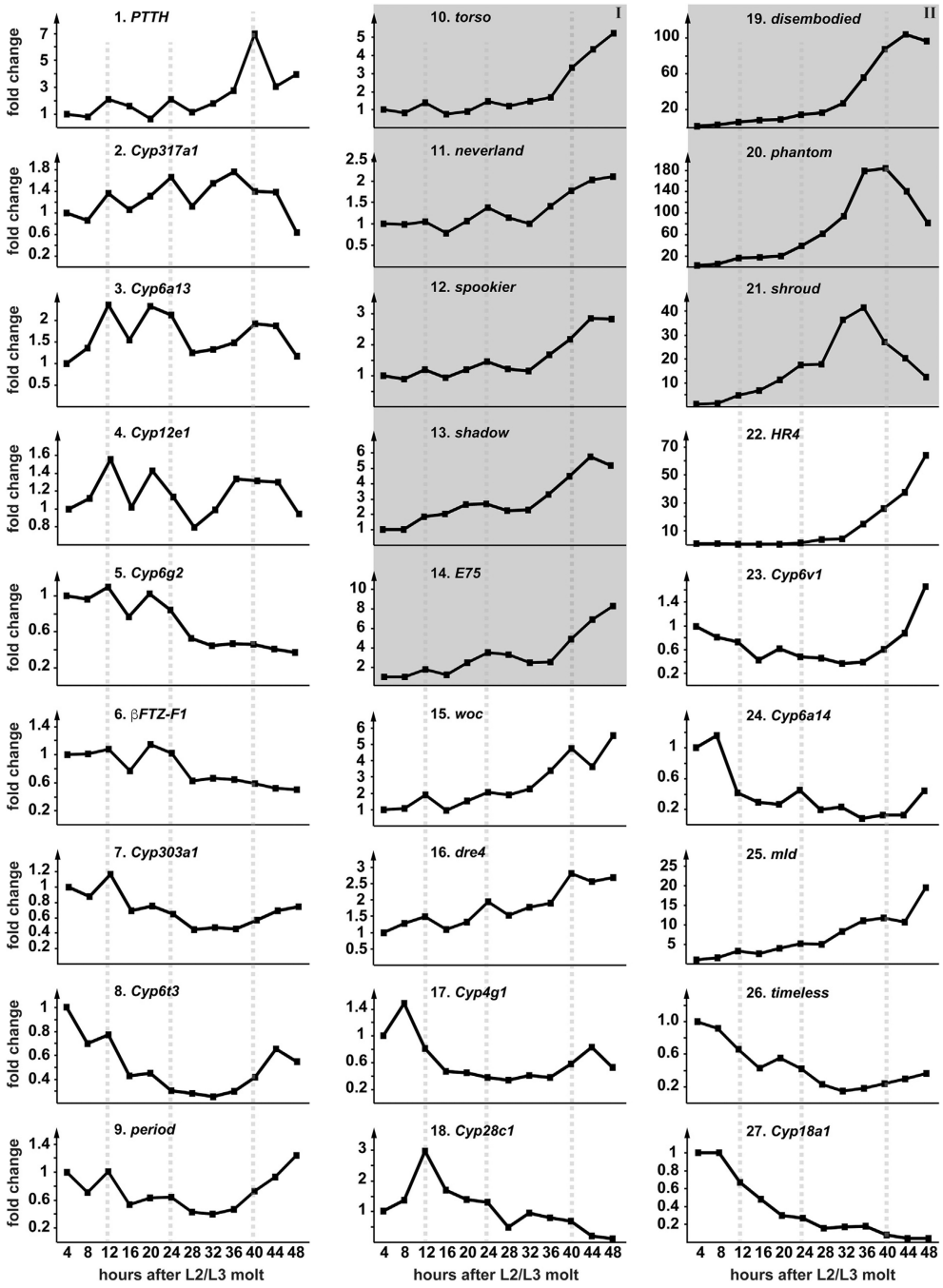

Figure 3. qPCR Time Course of Genes with Confirmed or Suspected Roles in Steroid Production

RNA isolated from BRGCs of carefully staged L3 larvae was subjected to microfluidic qPCR (Fluidigm). The 12 time points span nearly the entirety of the L3 stage, which lasts ~48 hr. The transcripts of PTTH oscillate, and the gray lines indicate the three peaks. The 4 hr time point served as calibrator and was normalized to 1 (grey boxes: reflect proposed class I and class II genes).

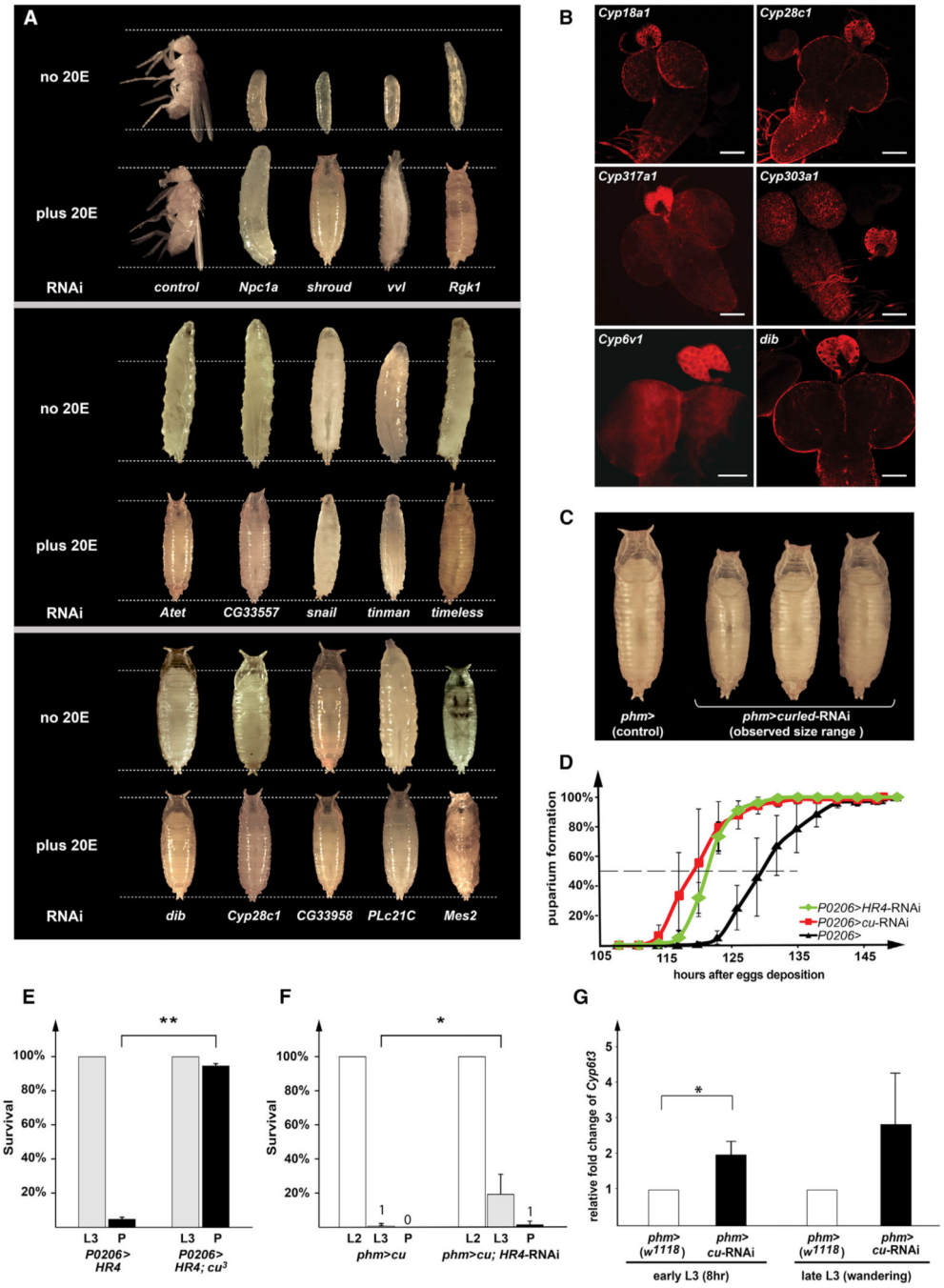

Figure 4. Genes Identified Here with Putative Functions in the PG

(A) Phenotypes of PG-specific RNAi and rescue with 20E. The dotted lines show the average maximal length of control L3 larvae. The controls develop normally in the absence or presence of dietary 20E (top left). RNAi: *phm22-Gal4* was used to induce RNAi in the PG. We included *dib* and *sro* as positive controls, which continued to develop into adults (only the pupal stage is shown for comparison).

(B) In situ hybridization for uncharacterized P450 genes with moderate to high RG-specific expression: *Cyp28c1, Cyp303a1, Cyp317a1*, and *Cyp6v1* (Table S1) (from 0–8 hr L3).

Cyp18a1 and *dib* served as controls for moderate and high RG specificity, respectively (from late L3). The scale bar represents 100 μm.

(C) PG-specific RNAi of *cu* reduced pupal body size. *phm>*: *phm-Gal4* alone.

(D) *cu*-RNAi causes developmental acceleration similar to *HR4*-RNAi (*P0206>*: RG-specific *Gal4* driver and hormone receptor 4: HR4). The dotted line indicates when 50% of the larval population has reached the prepupal stage.

(E) Genetic interaction between *HR4* and *cu: HR4*-cDNA is expressed in a control or *cu* mutant background. *P0206>HR4*: RG-specific Gal4 driving *UAS-HR4* cDNA; cu^{3}: null allele of *cu* (Grönke et al., 2009).

(F) Genetic interaction between *HR4* and *cu*, via expression of a *cu*-cDNA in a control or *HR4*-RNAi background. *phm>cu*: PG-specific expression of a *cu* cDNA.

(D and E) Percentage of animals reaching the second instar (L2, white), third instar (L3, gray), or pupal stage (P, black) (**$p < 0.01$ and *$p < 0.05$) (Student's t test and the error bars represent SD). The numbers in the graphs show the percentage of low-level survival.

(G) qPCR expression data for *Cyp6t3* (a target gene of HR4) in RGs isolated from controls (*phm>*w^{1118}) or PG-specifi cu-RNAi larvae (phm>cu-RNAi). The RGs were isolated at 8 hr after the molt and ~24 hr later (wandering stage). The error bars are 95% confidence intervals and *$p < 0.05$.

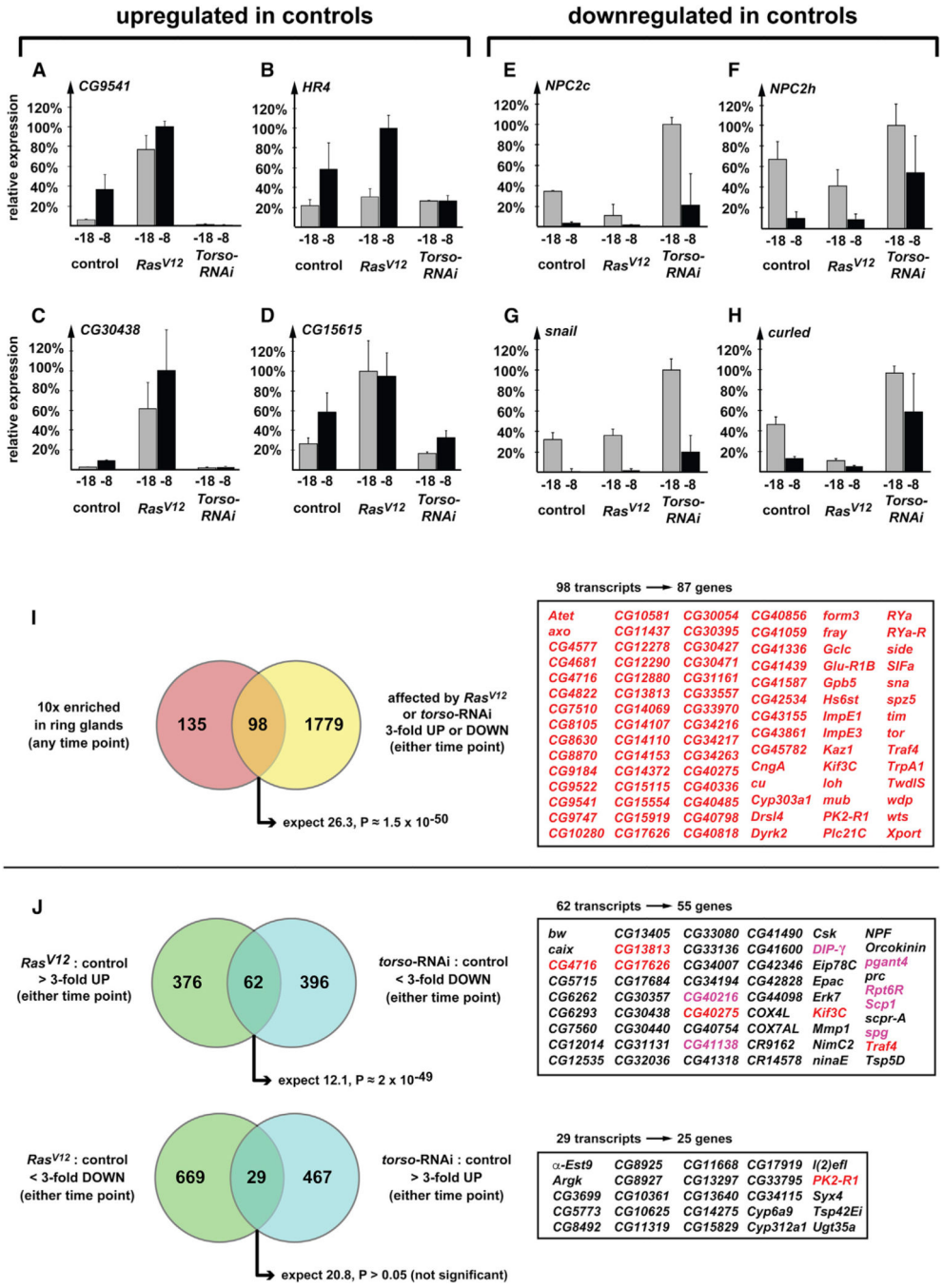

Figure 5. *Torso*-RNAi and *Ras*^{V12} Microarray Results

(A–H) Shown are representative genes that were either up- or downregulated between the −18 (gray) and −8 (black) hr time points in controls, representing low (−18) and elevated (−8) PTTH levels in controls (see Figure 1A). See Tables S8A and S8B for all genes that showed comparable profiles. The condition with the highest expression for a given gene was normalized to 100%. The error bars represent SD. The examples are provided for genes corresponding to RG-enriched transcripts (A, C, G, and H) (Figure 1B) and non-enriched transcripts (B and D–F) (control: *phm>w*^{1118}). *Ras*^{V12}: *phm>Ras*^{V12} expresses

constitutively active Ras (= active PTTH pathway in the PG). *torso*-RNAi: *phm>torso*-RNAi (= disrupted PTTH pathway in the PG).

(I and J) Number in circles reflect the total number of significantly affected transcripts, based on t test ($p < 0.01$) and fold change cutoff (I and J). To judge the relevance of overlapping gene sets, we calculated p values based on the $\chi 2$ test. The p values describe whether the difference between the observed and expected number of transcripts in the overlap is significant, where the expected number is the average overlap when two randomly generated lists (of the same size as the tested sets) from all *Drosophila* transcripts represented on the array are compared. The genes corresponding to the overlap are listed in the box, where red indicates >10-fold and purple represents moderate transcript enrichment (5- to 10-fold) in the RG.

(I) Venn diagram comparing 233 transcripts with 10-fold enrichment to 1,877 transcripts affected by the Ras^{V12} or *torso*-RNAi arrays.

(J) Venn diagrams testing for inverse correlation between upregulated transcripts from the Ras^{V12} array and downregulated transcripts from the *torso*-RNAi and vice versa.

Table 1

GOSTAT Results for 233 RG-Specific Transcripts

Receptor activity[a]	6.6×10^{-07}	*mthl6; Toll-4; mthl7; sevenless; PK2-R1; Glu-RIB; Ekar; star1; mthl12; CG33958; Ir41A; MstProx; torso; CG7497; RYa-R; Sr-CIII; CG12290; Hmu;* and *PROC-R*
Response to heat	1.5×10^{-06}	*Hsp70bc; Hsp70bb; Hsp70ab; hsp70ba;* and *hsp70bbb*
Sterol metabolic process	1.4×10^{-05}	*mld; dib; Npc1a; phm;* and *sad*
Hormone biosynthetic process	4.0×10^{-05}	*mld; dib; phm; sad;* and *jhamt*
Signal transduction	1.5×10^{-04}	*mthl6; Toll-4; mthl7; sevenless; PK2-R1; Pvf2; SIFa; Cng; Ext2; Traf4; star1; mthl12; Ir41a; torso; MstProx; CG7497; RYa-R; Hs6st; CG12290; Akh;* and *PROC-R*
Oxidoreductase activity	2.7×10^{-04}	*Fdx2; dib; phm; CG40160; neverland; CG40485; CG17691; Cyp6g2; sad; Cyp303a1; FASN3; CG9522; sro; Cyp28c1; CG9747; Cyp6a13; CG4716;* and *CG8630*
GPCR signaling pathway	2.7 × 10 −04	*mthl6; mthl7; PK2-R1; RYa-R; CG7497; CG12290; SIFa; Akh; PROC-R; star1;* and *mthl12*
Tube morphogenesis	3.1 × 10 −02	*Hs6st; esg; form3; torso; warts;* and *snail*

[a]Transcripts with >10-fold were analyzed by GOSTAT for GO term enrichment (Beissbarth and Speed, 2004). The table lists the GO term, the p value, and genes associated with the term according to GOSTAT.

Table 2

RNAi Lines Identified with RG GAL4 Drivers

Gene[a]	VDRC ID	Phenotypes (Strongest Line)	20E Rescue
Driver *phm22-Gal4* (PG)			
Atet	42750 and 100404[c]	large permanent L3, no pupae	attempt PF
CG5278	107919	large L3/pupae/adults	normal timing/size
CG11762/ouib	108919	L2 arrest	not tested
CG30471	100166	large L3/pupae, no adults	form adults
CG33557	23517, 23518, and 109868	large permanent L3, no pupae	attempt PF
CG33958	4978, 101861[c], and 106547	large L3/pupae/adults	normal timing/size
cu	25176, 45441, 45442, 45443, and 109759[c]	some small L3/P, form adults	no rescue
Cyp28c1	51073	large L3, few pupae	attempt PF
dib	101117	large L3, larval lethality	form adults
Hsp70Ba	50381 and 50382	L2 arrest, large L2, no L3 or pupae	attempt PF
Mes2	37782[c] and 109111	pupal lethality (normal size)	no rescue
MstProx	108034	~20% pupal lethality (slightly enlarged)	no rescue
Npc1a	105405	large L1, no later stages	wandering L3
phm	108359	L1 arrest	form adults
Plc21C	26557[c], 26558, and 108395	large L3/pupae/adults	normal timing/size[b]
Rgk1	30103 and 30104[c]	large L2, no later stages	form L3/P
sad	106356	large L3/pupae	form adults
sro	50111	large L1, no later stages	form adults
snail	6232[c],50003, and 50004	large permanent L3, no pupae	wandering L3
spz5	41295 and 102389	large permanent L3, no pupae	form adults
spok	51081	large L3/pupae	form adults
tinman	12655, 12656, 32510, and 101825[c]	large permanent L3, no pupae	wandering L3
tim	2885, 2886, and 101100	large permanent L3, no pupae	attempt PF
Ugt37c1	46514	embryonic lethality	no rescue
vvl	47182, 47185, and 110723	large L1, no later stages	form L2/L3
Driver:*Aug21-Gal4* (CA)			
Oatp74D	37295	~30–50% late pupal lethality	NA
Driver*Akh-Gal4* (CC)			
None of the above lines resulted in phenotypes when RNAi was expressed in the CC.			

[a] Of the 102 tested genes, we identified 25 hits in the PG and one hit in the CA. The phenotype of the strongest RNAi line is described.

[b] Plc21C with 20E forms no adults.

[c] No obvious phenotype with phm22-Gal4 driver.